LOW-TEMPERATURE TITANIA-GRAPHENE QUANTUM DOTS PASTE FOR FLEXIBLE DYE-SENSITISED SOLAR CELL APPLICATIONS

D. Kishore Kumar,[1] Damaris Suazo-Davila,[2] Desiree García-Torres,[2] Nathan P. Cook,[3] Aruna Ivaturi,[4] Min-Hung Hsu,[1] Angel A. Martí,[3] Carlos R. Cabrera,[2] Baixin Chen,[1] Nick Bennett,[1] and Hari M. Upadhyaya[5]*

[1]Energy Conversion Lab (ECL), Institute of Mechanical Process and Energy Engineering (IMPEE), School of Engineering and Physical Sciences, Heriot-Watt University, Riccarton, Edinburgh, EH14 4AS, UK.

[2]Department of Chemistry and NASA Center for Advanced Nanoscale Materials, University of Puerto Rico, Rio Piedras Campus, San Juan, Puerto Rico 00931-3346, USA.

[3]Department of Chemistry and Department of Bioengineering, Rice University, Houston TX 77005, USA.

[4]Department of Pure and Applied Chemistry, University of Strathclyde, Glasgow, G1 1XL, UK.

[5]Advanced Materials Centre, School of Engineering, London South Bank University, 103, Borough Road, London- SE10 AA, UK.

Key words: Graphene quantum dots, binder free TiO_2 paste, polymer substrate, DSSC.

*Corresponding author: D. Kishore Kumar, Energy conversion lab, Institute of Mechanical Process and Energy Engineering, School of Engineering and Physical Sciences, Heriot-Watt University, Riccarton, Edinburgh, EH14 4AS, Scotland, UK. Email id: nanokishore@gmail.com

Abstract

Graphene possesses excellent mechanical strength and chemical inertness with high intrinsic carrier mobility and superior flexibility making them exceptional candidates for optoelectronic applications. Graphene quantum dots (GQDs) derived from graphene domains have been widely explored to study their photoluminescence properties which can be tuned by size. GQDs are biocompatible, low cytotoxic, strongly luminescent and disperse well in polar and non-polar solvents showing bright promise for the integration into devices for bioimaging, light emitting and photovoltaic applications. In the present study, graphene quantum dots were synthesized by an electrochemical cyclic voltammetry technique using reduced graphene oxide (rGO). GQDs have been incorporated into binder free TiO_2 paste and studied as a photoelectrode material fabricated on ITO/PEN substrates for flexible dye sensitized solar cells (DSSCs). DSSC based on GQDs-TiO_2 exhibited open circuit output potential difference (V_{oc}) of 0.73 V, and short circuit current density (J_{sc}) of 11.54 mA cm^{-2} with an increment in power conversion efficiency by 5.48 %, when compared with those with DSSC build with just a TiO_2 photoanode (open-circuit output potential difference (V_{oc}) of 0.68 V and short circuit density (J_{sc}) of 10.67 mA cm^{-2}). The results have been understood in terms of increased charge extraction and reduced recombination losses upon GQDs incorporation.

1. Introduction

With the advent of nanotechnology, advanced carbonaceous materials of nanoscale size with unique properties were discovered in succession, with buckminsterfullerene C_{60} in 1985,[1] carbon nanotubes in 1991,[2] and most recently graphene in 2004.[3] Graphene is a two dimensional material possessing excellent mechanical strength,[4] and chemical inertness with high intrinsic carrier mobility,[5] and excellent flexibility.[6] Graphene has been used as an electron acceptor material in photovoltaics due to its high electron mobility.[7] The dispersion of graphene is poor in commonly used solvents and this has been an inhibiting factor for the practical applications of graphene.[8] In the past few years, there has been enthusiasm to convert graphene to 0-dimension graphene quantum dots (GQDs) and to study phenomena such edge and size effects on GQD properties.[9] These GQDs are usually biocompatible, strongly luminescent and can dispersed well in various solvents being promising prospects for integration into bioimaging devices,[10] light emitting,[11] and photovoltaic applications.[12]

The utilization of graphene for different applications could be facilitated by tuning the band-gap of graphene which is achieved by converting them into GQDs. It has been reported that the graphene-TiO_2 composite exhibits high photoconversion efficiency. To explore GQDs properties such as quantum confinement, edge effects, strong luminescence and many others, we were interested studying a GQDs-TiO_2 composite as photoanode in polymer based flexible DSSC. In addition to these, the GQDs acts as a good electron acceptor, exhibit weak molecular interaction for dye molecule and co-sensitization improves charge collection efficiencies.[13]

Many synthetic procedures have been reported for the synthesis of GQDs in the literature. Khalid Habiba *et al.* reported the pulse laser synthesis of GQDs by 1024 nm pulsed Nd:YAG

laser using benzene as precursor material in presence of a NiO catalyst and investigated their suitability as biomarkers.[14] Lijie Kou *et al.* reported the synthesis by breaking the acid functionalization of double walled carbon nanotubes into graphene nanosheets and later into GQDs for application in flexible memory devices.[15] Yan Li *et al.* developed an efficient and direct preparation of GQDs by electrochemical cyclic voltammetry using graphene as a precursor.[16] Yongqiang Dong *et al.* synthesized GQDs by a simple method where in citric acid was pyrolyzed at 200 °C for 30 minutes. The final yield of the GQDs reported in this study was about 10 %.[17] Xin Yan *et al.* communicated the synthetic route of synthesizing GQDs by using a polyphenylene dendritic precursor.[18] Shoujun Zhu *et al.* described the synthesis of GQDs by a solvothermal route using graphene oxide as a starting material for bioimaging of MG-63 cells.[19] Jianhua Shen *et al.* and Dengyu Pan *et al* reported the synthesis of GQDs by a hydrothermal method using graphene oxide as the starting material.[20] Libin Tang *et al.* described the GQDs synthesis by microwave irradiation using glucose and demonstrated their application in conversion of blue light into white light.[21] S. Schnez *et al.* demonstrated the synthesis of GQDs by designing the desired shape and size using electron beam lithography for studying transport properties.[22] Ponomarenka *et al,* fabricated a single electron transistor using a graphene quantum dot of 30 nm synthesized by electron beam lithography.[23] It is evident that poor yield and expensive method were the major disadvantages in the preparation of GQDs.

The first application of GQDs in photovoltaics has been demonstrated in poly (3-hexylthiophene) (P3HT) based organic solar cells with the efficiency of 1.28 %.[16] GQDs are also reported in DSSCs, there are many reports available on the incorporation of GQDs in the preparation of photoanode for DSSC which are summarised in detail in Table 1.

To the best of our knowledge no reports are available on the incorporation of GQDs in binder free TiO_2 paste for application of flexible DSSCs. In this work, we report on the synthesis of the graphene quantum dots by the electrochemical cyclic voltammetry technique. Binder free TiO_2 paste is prepared using GQDs and *tert*-butyl alcohol in dilute acidic medium. GQDs-TiO_2 paste has been used in the fabrication of flexible polymer DSSC and exhibited an efficiency of 4.41 %.

2. Experimental Techniques

2.1. Synthesis of Graphene oxide

In the present study all the chemicals were procured from Sigma-Aldrich and Fisher and used without any further purification. Graphene oxide (GO) was synthesized by the modified Hummer's method.[24] In this method, 2 g of graphite flakes were mixed with 1g of $NaNO_3$ and treated with 100 mL of concentrated H_2SO_4 at 0 °C for 30 min. Then 12 g of $KMnO_4$ was added to this solution while the temperature of the solution was maintained below 30 °C. After refluxing for 6 h, the mixture was diluted with DI water (500 mL) containing 10 mL of 30 % H_2O_2 to neutralize the excess $KMnO_4$. Finally, the mixture was washed several times with 1.0 L of 1 M HCl and followed by deionized water. After drying at 60 °C overnight, GO was re-dispersed in DI water, sonicated for 10 min and centrifuged at 4000 rpm to remove unexfoliated GO. The GO solution was drop casted on a p-Si/SiO_2 substrate and placed horizontal tube furnace equipped with Ar-H_2 gas supply and annealed at 600 °C with heating rate of 30 °C/min to transform the material into reduced graphene oxide (rGO).

2.2. Synthesis of Graphene Quantum Dots

GQDs were synthesized using the electrochemical cyclic voltammetry technique.[7] The rGO film on the p-Si/SiO_2 substrate was used as the working electrode and platinum wire as the counter electrode. The reference electrode was E vs (Ag/AgCl)/V and the electrolyte was 0.5 M sodium phosphate buffer solution of pH 6.8. The potential window of the voltammogram (Metrohm Autolab PGSTAT30) was recorded from -3.0 V to 3.0 V for 2000 cycles. After the completion of cyclic voltammetry cycles, the washings of the rGO substrate and the electrolyte were transferred to a MD 8000-10000 dialysis membrane. The dialysis was carried for two days with frequently changing DI water. Finally, the solution was concentrated by freeze-drying.

2.3. Procedure for assembling the DSSC

Room temperature binder-free TiO_2 paste,[25] was prepared by refluxing 0.2 g of Degussa P25 TiO_2 nanoparticles and 1.4 mL of tert-butyl alcohol in 0.2 mL of 0.05 M HNO_3 medium with addition of 0.5 mL of the GQDs dispersion. The contents were stirred for 8 h at room temperature. The TiO_2 films are prepared by doctor blade technique on ITO/PEN films (Peccells, Japan). After each coating, the films were subjected to flash annealing for 2 min at 175 °C. Similarly, TiO_2 films were prepared from GQDs free TiO_2 paste which was prepared by adding 0.5 mL of deionised water instead of GQDs solution. Then the films were soaked in 0.1 mM N719 in absolute ethanol (Dyesol) dye bath for 20 h.

The DSSC was assembled by joining the photoanode with platinum coated ITO/PEN counter electrode (Peccells, Japan) using 25 μm Surlyn (Solarnix) as the spacer. The electrolyte was injected from the platinum face through a hole that was drilled manually before assembling the DSSC. The electrolyte was comprised of 0.4 M lithium iodide (LiI), 0.4 M

tetrabutylammoniumiodide, 0.04 M iodine, and 0.3 M methylbenzimidazole in a mixture of acetonitrile and 3-methoxy propionitrile (MPN) of ratio of 1:1 (v/v).

2.4. Characterisation Techniques

The phase purity and crystallographic structure of GO, rGO and GQDs were determined using an automated Rigaku D/max 2400 X-ray diffractometer with rotating anode using Cu Kα radiation (0.15416 nm). The graphene oxide was dispersed on the standard copper metal sample holder and the measurement was recorded from 5 ° to 30 ° at a scan rate of 3 °/min. Absorbance spectra were recorded using Shimadzu 2450 UV-Vis spectrophotometer and photoluminescence excitation and emission spectra were recorded using HORIBA Jobin Yvon FluoroLog 3 fluorometer. The lifetime decay measurements were obtained by using Edinburgh Instruments OD470 single-photon counting spectrometer using a 371 nm picosecond pulse diode laser with a high-speed red detector. Raman spectra were collected on Horiba Jobin-YvonT-6400 Raman microprobe with a Coherent Innova99 Ar^+ laser at a wavelength of 514.5 nm. Structural and morphology investigations are carried using a transmission electron microscope JEOL JEM-2200FS operated at 200 kV and a scanning electron microscopy FESEM JEOL JSM-7500F, respectively. J-V measurements were carried with Newport 92250A-1000 Solar Simulator under AM1.5G conditions. The electrochemical impedance spectroscopy (EIS) were carried out using Metrohm Autolab PGSTAT30 with amplitude signal of 50 mV in the frequency range of 1 MHz to 0.1 Hz at -0.7 V in the dark.

3. Results and Discussions

3.1. Structural, optical and morphological characterisation of graphene quantum dots

3.1.1. X-ray Diffraction studies

Fig. 1 shows XRD profiles of the GO (green), rGO (black) and GQDs (red) samples. The peak at 2θ = 9.48 ° (d = 0.93 nm) in the green curve corresponding to the (001) orientation and confirms the presence of GO.[26] On the other hand, there is a broad peak at 2θ = 26.3 ° (d = 0.34 nm) in the black curve corresponding to the (002) orientation revealing that the graphene oxide lost oxygen molecules during the transformation into reduced form.[27] In the XRD plot for GQDs (red curve), the position of (002) peak is shifted to lower 2θ to 26.11 ° (d = 0.34 nm) and the peak is also broadened when compared to rGO (black curve). When compared to graphene, GQDs have a broader XRD peak and this indicates that an electrochemical process has introduced more active sites on the GQD surface.[16]

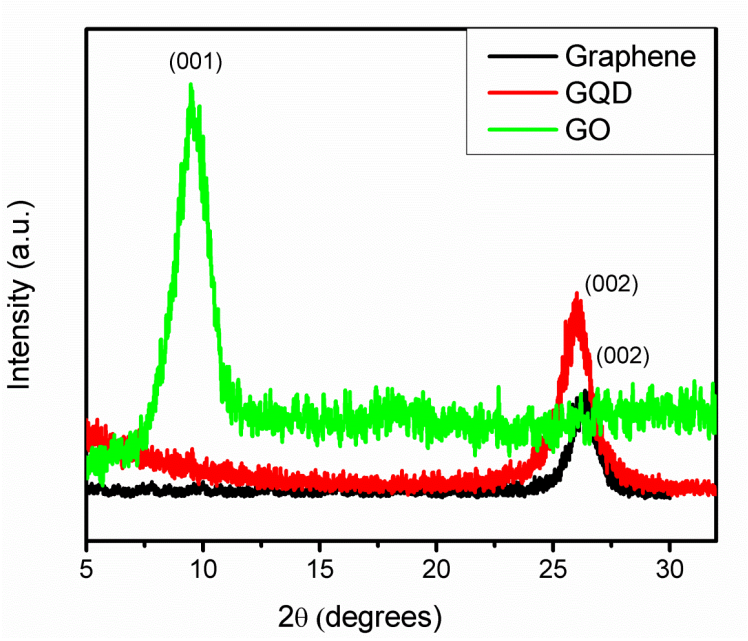

Fig. 1: X-ray diffraction (XRD) pattern of GO [2θ = 9.48° corresponds to the (001) planes], rGO [2θ = 26.3° corresponds to the (002) planes] and GQDs (2θ = 26.11° corresponds to the (002) planes].

3.1.2. Raman Spectroscopy

Raman scattering is a strong, powerful non-invasive and essential tool to characterize graphite and graphene related materials. Graphene and its related materials are allotrope forms of carbon. From the molecular perspective, these carbon allotropes are composed with C- C bonds. Nonetheless, in these allotropes, the hybridization of these bonds can differ. Raman spectroscopy is a powerful and sensitive technique for the characterisation of carbon allotropes and can detect slight modifications in C- C bonds.[28] In Fig. 2, the peak at 1351 cm^{-1} is related to the D-band and corresponds to the A_{1g} mode which represents the vibrations of carbon atoms with dangling bonds of disordered graphite. The presence of the G-band at 1592 cm^{-1} corresponds to the E_{2g} mode of graphite which in turn is related to the vibration of the sp2 bonded carbon atoms. From comparison of the Raman spectrum of GO and rGO it is evident that the thermal treatment of GO results in the change in intensities of the D-band and the G-band pre- and post-treatment. The ratio of relative intensities of D band and G band in GO was 1.24 indicating the presence of high proportion of defects and edge functional groups.[29]

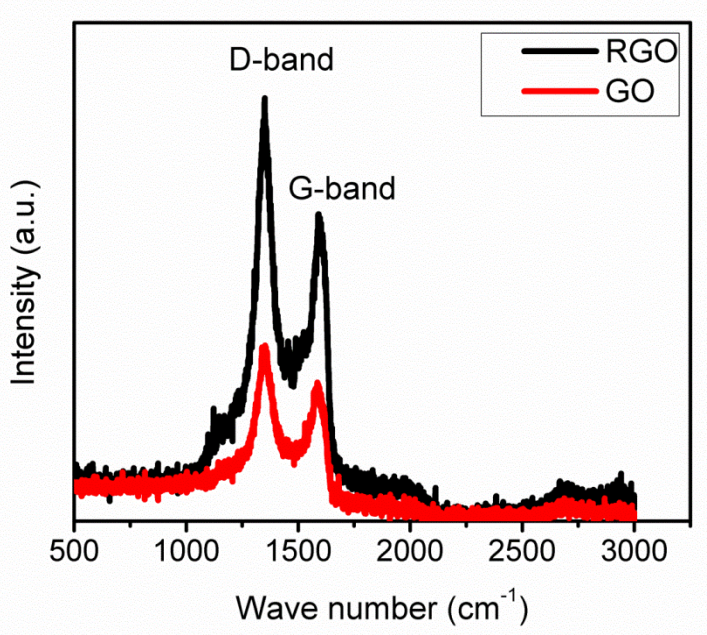

Fig. 2: Raman spectrum of GO and rGO represents D band at 1351 cm^{-1} and G band at 1592 cm^{-1}.

After thermal treatment, the G-band has become broader compared to GO and the ratio of the D/G intensity of rGO has been slightly increased to 1.38. This phenomenon can be explained due to the change in the sp2 domains due to oxidation and exfoliation, and partially disordered graphite crystal structure of graphene films after reduction.[30]

3.1.3. UV-Vis Absorption spectroscopy

Fig. 3 shows the UV-Vis spectrum of the GQDs solution. The absorbance is recorded in the range of 200 nm to 500 nm. In the spectrum, a shoulder at 270 nm (4.55 eV) is observed because of the interband transitions of the graphene sheet and excitonic effects.[31] This is a characteristic feature of the GQDs.

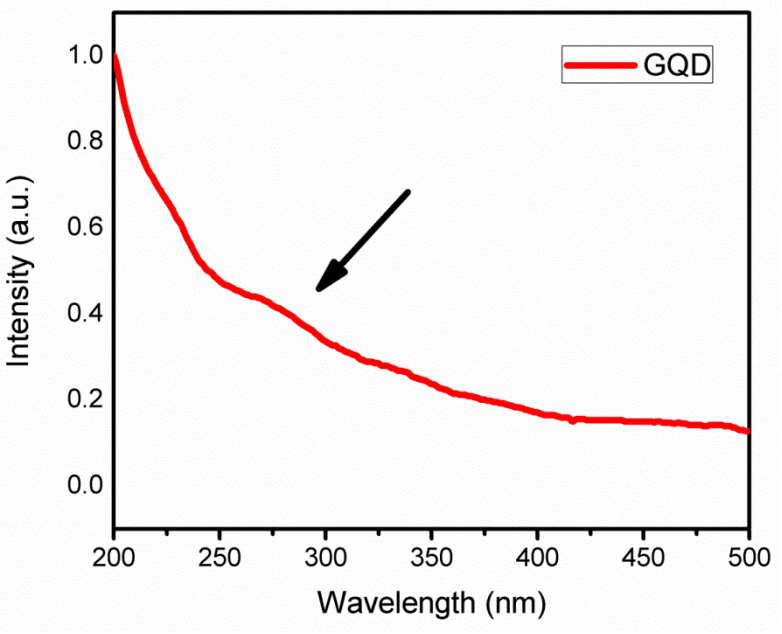

Fig. 3: UV-Vis absorption spectrum of GQDs exhibiting characteristic shoulder at 270nm.

3.1.4. Photoluminescence spectroscopy

Fig. 4 shows the photoluminescence (PL) spectra of GQDs. The sample is subjected to excitation in the range of 300 nm to 372 nm with interval of 8 nm. The emission peaks are observed in the range 420 nm to 450 nm. With the increase in the excitation wavelength the photoluminescence peak increases in intensity and shifts to higher wavelength, reaches a maximum at 430 nm corresponding to the excitation wavelength of 340 nm. For excitation wavelength greater than 340 nm, the PL emission peak decreases in intensity and shifts to higher wavelength range. It has been reported that the recombination of electron-hole pairs in the sp^2 clusters leads to PL emission in the carbonous materials,[32] and PL emission of the GQDs follows an excitation dependent feature which is commonly observed in carbon materials.[19]

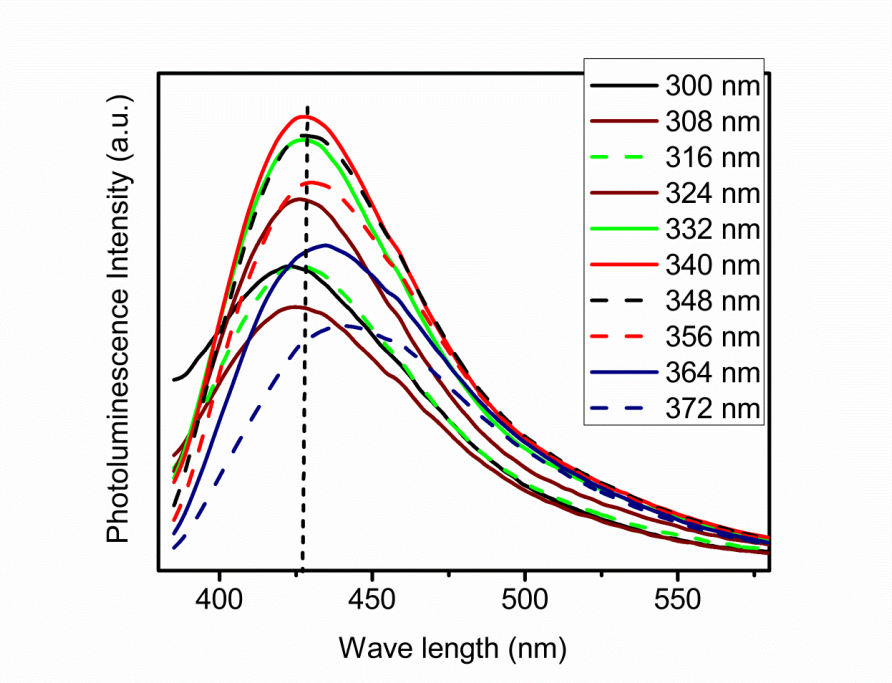

Fig. 4: Photoluminescence spectra of GQDs in water excited at wavelengths from 300 nm to 372 nm with intervals of 8 nm.

In Fig. 5, the decay of the emissive state in GQDs is studied by time resolved luminescence fluorescence decay after excitation with a wavelength of picosecond 371 nm laser pulse. The photoluminescence decay is biexponential having a short (τ_1) and long (τ_2) lifetime components.[33] The multi-exponential life time is associated with a variety of factors that can include band to band transitions, the presence of defect sites, and edge functionalities.[34] The average lifetime decay value is found to be 4.8 ns which is well comparable to the literature reports.[35,36]

τ_1=1.98±0.03 ns (40%).....(3)

τ_2=7.37±0.05 ns (60%).....(4)

Average lifetime = 4.8 ns

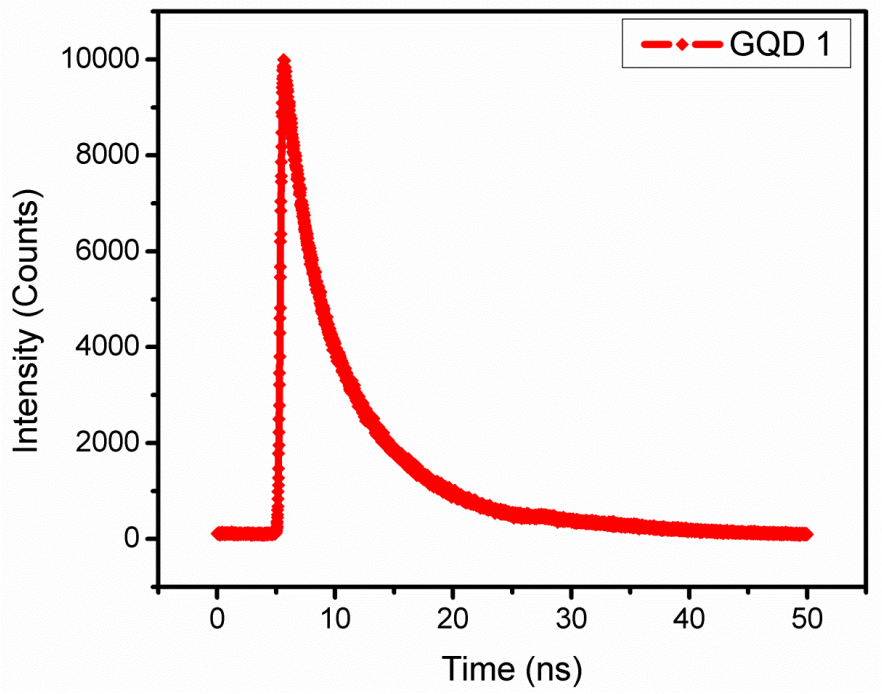

Fig. 5: Life time decay studies of GQDs in DI water.

3.1.5. Morphology studies by SEM and HR-TEM of Graphene quantum dots

The rGO SEM micrographs are shown in Fig. 6. Free standing rGO are obtained after thermal reduction of GO.

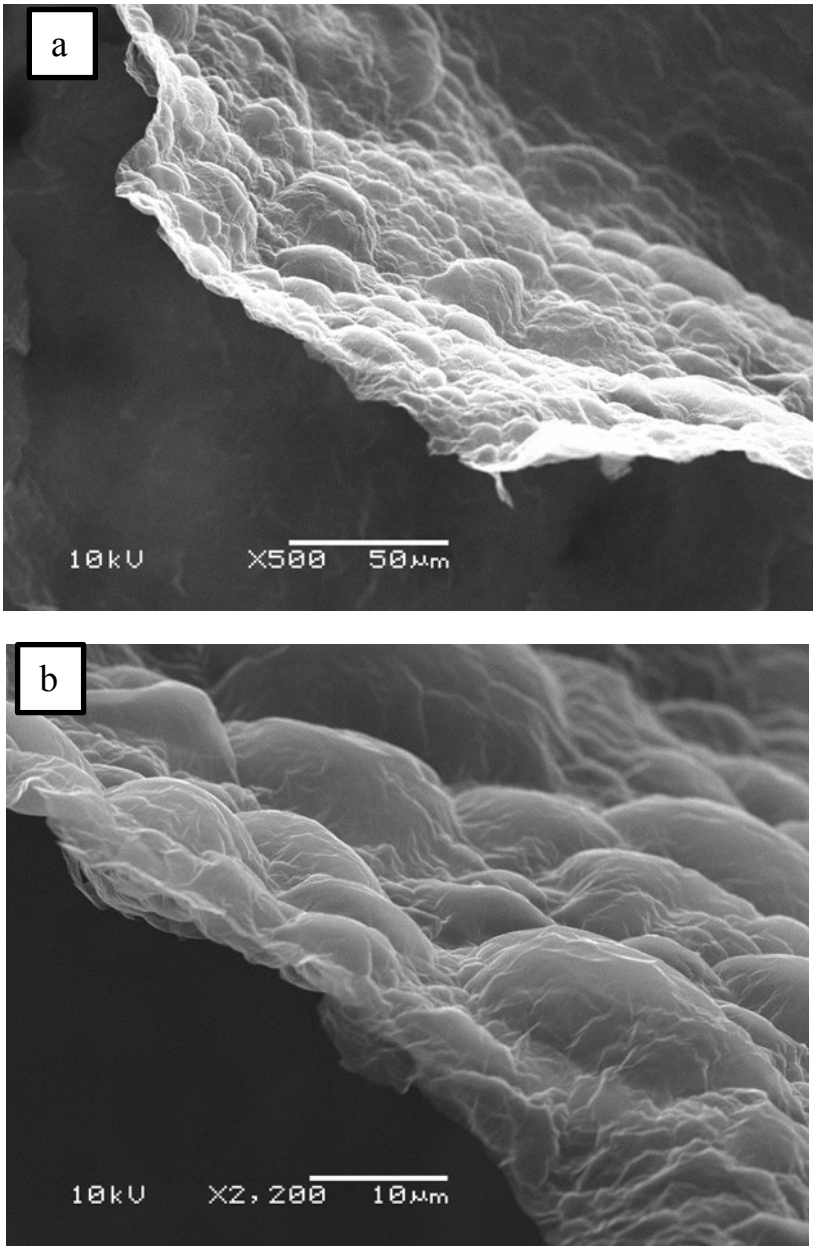

Fig. 6: SEM micrographs of rGO a) lower magnification b) higher magnification images, ripples on the surface of rGO indicate the presence of surface defects due to oxygen vacancies.

The formation of ripples on surface of the rGO provides evidence of surface defects which are created by the oxygen vacancies and supported by the presence of a D-band in the Raman spectra (Fig. 2).[37] HR-TEM is employed to investigate the size distribution of GQDs. The samples are prepared by pipetting few micro litres of GQDs solution on a mica grid. In Fig. 7, HR-TEM micrographs reveals that the GQDs are about 2-3 nm in size and the fringe width is 0.21 nm which is in agreement with literature.[38]

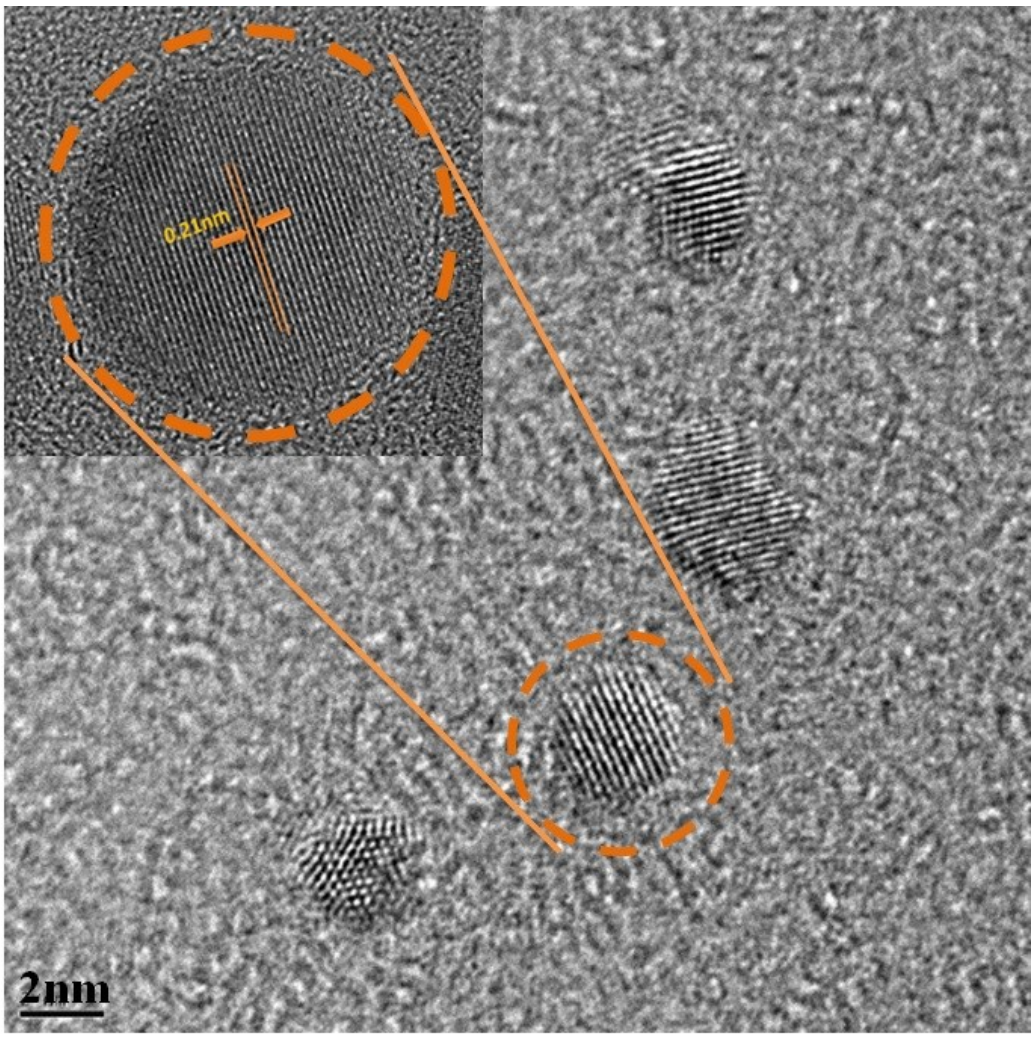

Fig. 7: HRTEM micrographs of GQDs and inset indicate the GQDs of sizes of 2-3 nm.

3.2. Photovoltaic properties of GQDs based polymer flexible DSSC

The J-V characteristics of champion TiO_2 cells and GQDs-TiO_2 cells prepared on a PEN/ITO flexible foil are shown in Fig. 8. The solar cell characteristics of these devices are summarised in Table. 1. The results clearly shows that DSSC fabricated using GQDs-TiO_2 paste displays a better performance with improved short circuit current density (J_{sc}) of 11.54 mA cm^{-2}, better open circuit output potential difference (V_{oc}) of 0.73 V and power conversion efficiency (PCE) of 4.43 % when compared to GQDs- free TiO_2 paste. Although the overall conversion efficiency increase appears less, there has been significant increase in both the photocurrent and photo output potential difference parameters of the solar cell. It is evident that incorporation of GQDs into TiO_2 increases the photovoltaic parameters of the cells.

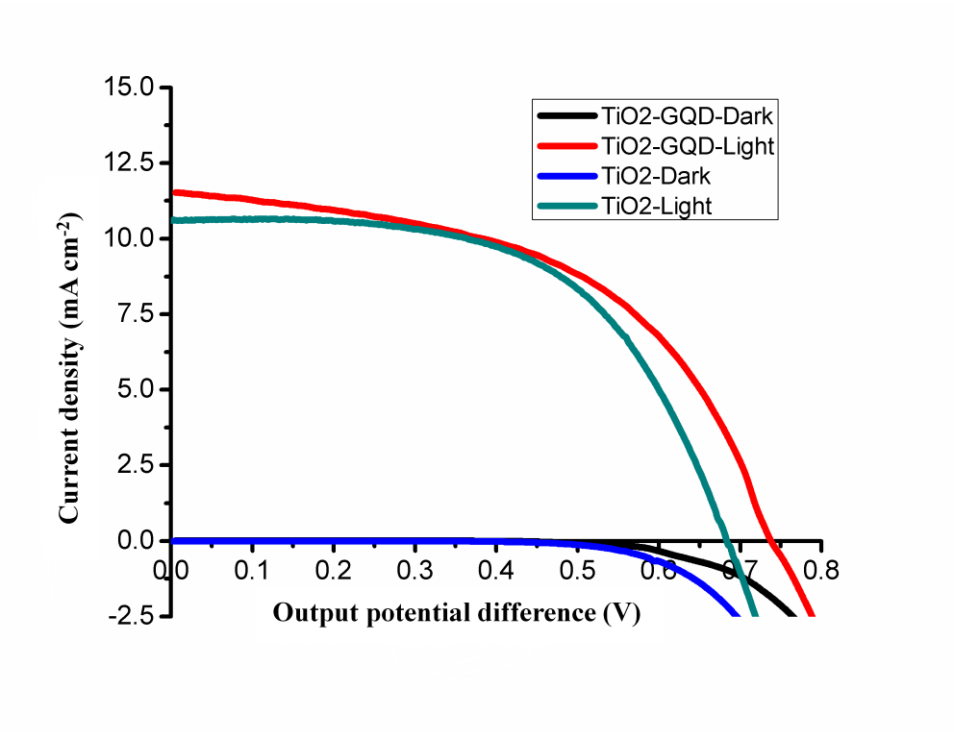

Fig. 8: J-V characteristics of flexible solar cell made with binder free GQD-TiO_2 paste (red curve in presence of light and black in dark condition) and TiO_2 paste (dark cyan curve in presence of light and blue in the dark) recorded under simulated AM1.5G.

Table.1: Photovoltaic performances of DSSCs devices fabricated with GQDs as photoelectrode.

S. No.	Substrate used	Structure	Method for GQDs	Photoanode process temperature	V_{oc} (V)	J_{sc} (mA cm^{-2})	FF (%)	η (%)	Ref
1	FTO glass	FTO/TiO_2/GQDs/D719/I^-:I_3^-/Pt/FTO	Spin coating	450 °C	0.77	15.20	75.0	7.95	[39]
2	FTO glass	FTO/TiO_2/GQDs/N719/ I^-:I_3^-/Pt/FTO	Physical adsorption	500 °C	0.66	14.07	59.0	6.1	[40]
3	FTO glass	FTO/ZnO/N719/GQDs/ I^-:I_3^-/Pt/FTO	Physical adsorption	450 °C	0.71	1.29	66.3	0.6	[41]
4	FTO glass	FTO/TiO_2/GQDs/N3/ I^-:I_3^-/Pt/FTO	Physical adsorption	450 °C	0.58	5.58	66.0	2.15	[42]
5	FTO glass	FTO/TiO_2/GQDs/N719/ I^-:I_3^-/Pt/FTO	Electrophoretic filling	450 °C	0.68	11.72	78.0	6.22	[43]
6	FTO glass	FTO/TiO_2/N719/GQDs/ I^-:I_3^-/Pt/FTO	Physical adsorption	450 °C	0.77	16.64	63.0	7.96	[44]
7	FTO glass	FTO/GQDs/N719/ I^-/I_3^-/Pt/FTO	Physical adsorption	500 °C	0.79	22.6	70.0	11.7	[45]
8	ITO glass	ITO/Pani-GQDs/N719/ I^-/I_3^-/Al	Drop casting	-	0.65	7.35	65.4	3.12	[46]
9	ITO glass	ITO/PPy-GQDs/N719/ I^-/I_3^-/Graphite/ITO	Drop casting	-	0.54	7.80	50.0	2.09	[47]
10	ITO/ PEN	ITO/ TiO2/ N719/ I^-/I_3^-/Pt/ITO	Doctor blade	175 °C	0.68	10.67	57.7	4.2	[25]
11	ITO/ PEN	ITO/ GQDs-TiO2/ N719/ I^-/I_3^-/Pt/ITO	Doctor blade	175 °C	0.73	11.54	52.7	4.4	*

*this work

3.3. Electrochemical Impedance Spectroscopy (EIS)

In all electrical devices, the transport and recombination processes of electrons at various interfaces can be studied using EIS. In DSSC, mainly three interfaces (TiO_2/electrolyte, CE/electrolyte and electrolyte diffusion) play important roles in the device performance. In the Nyquist plots, the first semi-circle corresponds to the counter electrode/electrolyte interface, the second semi-circle is related to the charge transfer resistance at the TiO_2/electrolyte interface and

third semi-circle is due to the electrolyte/electrolyte diffusion.[48] In the Nyquist plot (Fig. 9), the radius of the semi-circles was different.

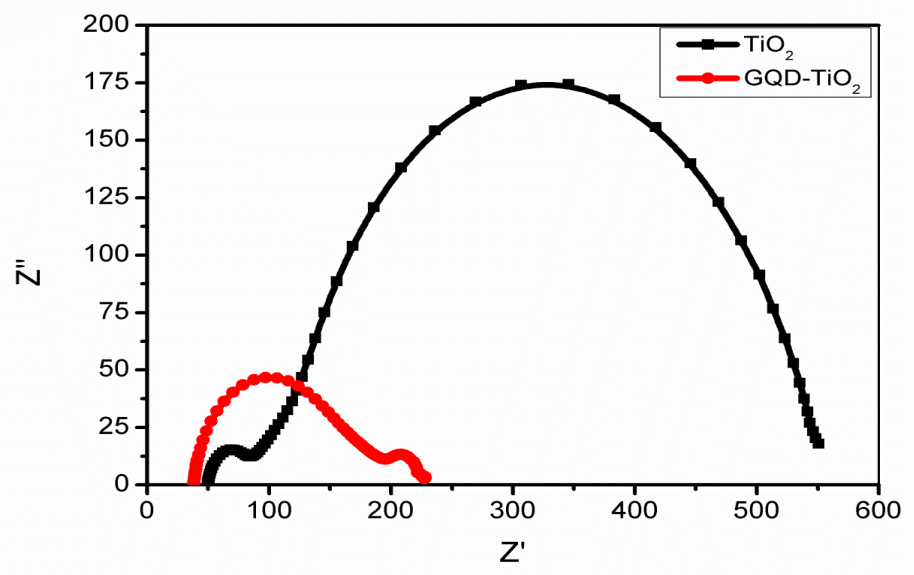

Fig. 9: Nyquist plots of GQDs-TiO_2 (red colour) and TiO_2 (black colour) cells measured at -0.7 V in dark condition.

The charge transfer resistance of TiO_2/electrolyte is low in the case of GQDs-TiO_2 paste and high in the case of TiO_2 paste. It is evident that the recombination of electrons in the TiO_2/electrolyte interface is diminished with the incorporation of GQDs in the TiO_2 paste. The life time of the electron is calculated using the expression from the Bode phase shown in Fig. 10,

$$\tau = 1/2\pi f_{max} \ldots\ldots\ldots\ldots (5)$$

where τ is the lifetime of the electron in the TiO_2/electrolyte interface and f_{max} is the maxima of the middle frequency peak in the Bode plots.[49] The life time of the electron in the GQDs-TiO_2/interface is 68.05 ms whereas, in TiO_2/electrolyte it is 44.28 ms. From the life time measurements, it is observed that GQDs-TiO_2 exhibited longer life-time than TiO_2. The longer electron life-time was attributed to reduced recombination between TiO_2 and the electrolyte

interface. Also, longer life-time is also related with improved charge transport.[50] Thus longer life times of electrons in DSSC are the key parameters in the improvement in the J_{sc} and V_{oc}.[51]

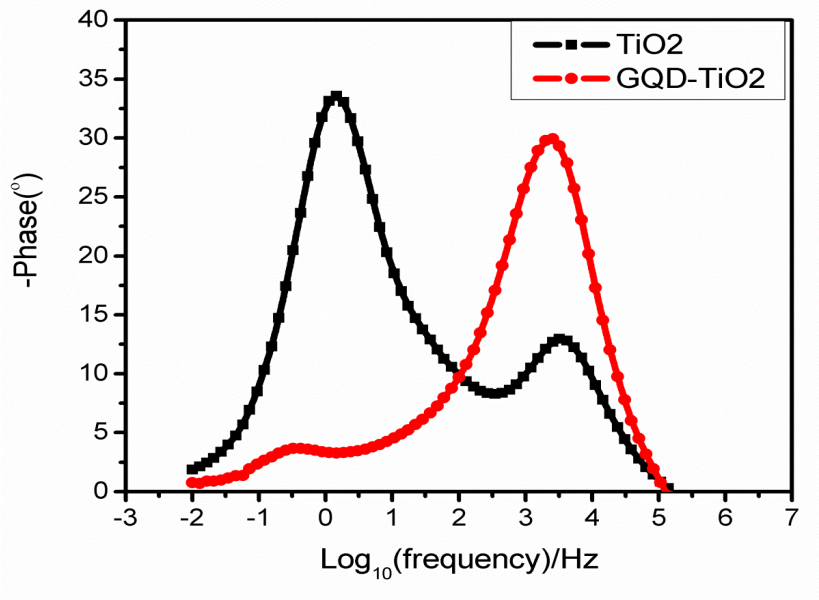

Fig. 10: Bode-modulus phase plots of GQDs-TiO_2 and TiO_2 cells recorded at -0.7 V under dark conditions.

4. Conclusions

In summary, the experiment of adding graphene quantum dots in room temperature binder free TiO_2 paste has yielded promising results. Although limited improvement was observed in photoconversion efficiency (4.2 % to 4.43 %), relatively better photocurrent and photo output potential difference increase has been observed. Further experiments carried out to measure the impedance spectroscopy have shown increase in life time (44.28 ms to 68.05 ms). GQDs have been prepared by electrochemical cyclic voltammetry technique using reduced graphene oxide as starting material. By using GQDs, the room temperature binder free TiO_2 paste was prepared with tert-butyl alcohol in dilute acidic medium and films were made by

doctor blade method on ITO coated PEN substrates. These results clearly indicate that GQDs plays a significant role in the performance of the DSSC and has plenty of room for improvement of the photoconversion parameters. This work leads to a promising application of GQDs in the hybrid photovoltaics.

Acknowledgement

The authors thank the EPRSC-DST APEX consortium grant number EP/H040218/1 for the financial support.

Declaration of interests:

The authors declare no competing interests.

References

[1] H. W. Kroto, J. R. Heath, S. C. O'Brien, R. F. Curl, R. E. Smalley, C60: Buckminsterfullerene, Nature 318 (1985) 162- 163.

[2] S. Iijima, Helical microtubules of graphitic carbon, Nature 354 (1991) 56-58.

[3] K. S. Novoselov, A. K. Geim1, S. V. Morozov, D. Jiang, Y. Zhang, S. V. Dubonos, I. V. Grigorieva, A. A. Firsov, Electric field effect in atomically thin carbon films, Science 306 (2004) 666-669.

[4] T. J. Booth, P. Blake, R. R. Nair, D. Jiang, E. W. Hill, U. Bangert, A. Bleloch, M. Gass, K. S. Novoselov, M. I. Katsnelson and A. K. Geim, Macroscopic graphene membranes and their extraordinary stiffness, Nano Lett. 8 (2008) 2442-2446.

[5] K. I. Bolotin, K. J. Sikes, Z. Jiang, M. Klima, G. Fudenberg, J. Hone, P. Kim, H. L. Stormer, Ultrahigh electron mobility in suspended graphene, Solid State Commun. 146 (2008) 351-355.

[6] Z. Dong, C. Jiang, H. Cheng, Y. Zhao, G. Shi, L. Jiang, L. Qu, Facile fabrication of light, flexible and multifunctional graphene fibers, Adv. Mater. 24 (2012) 1856-1861.

[7] Z. Liu, Q. Liu, Y. Huang, Y. Ma, S. Yin, X. Zhang, W. Sun, Y. Chen, Organic Photovoltaic Devices Based on a Novel Acceptor Material: Graphene, Adv. Mater. 20 (2008) 3924-3930.

[8] S. Stankovich, D. A. Dikin, R. D. Piner, K. A. Kohlhaas, A. Kleinhammes , Y. Jia, Y. Wu, S. T. Nguyen, R. S. Ruoff, Synthesis of graphene-based nanosheets via chemical reduction of exfoliated graphite oxide, Carbon 45 (2007) 1558-1565.

[9] K. A. Ritter and J. W. Lyding, The influence of edge structure on the electronic properties of graphene quantum dots and nanoribbons, Nat. Mater. 8 (2009) 235-242.

[10] C. Chung, Y-K. Kim, D. Shin, S-R. Ryoo, B. H. Hong, and D-H. Min, Biomedical applications of graphene and graphene oxide, Acc. Chem. Res. 46 (2013) 2211-2224.

[11] T-H. Han, Y. Lee, M-R. Choi, S-H. Woo, S-H. Bae, B. H. Hong, J-H. Ahn & T-W. Lee, Extremely efficient flexible organic light-emitting diodes with modified graphene anode, Nat. Photon. 6 (2012) 105-110 & J. Wu, M. Agrawal, H. A. Becerril, Z. Bao, Z. Liu, Y. Chen and P. Peumans, Organic Light-Emitting Diodes on Solution-Processed Graphene Transparent Electrodes, ACS Nano 4 (2010) 43-48.

[12] J. T-W. Wang, J. M. Ball, E. M. Barea, A. Abate, J. A. Alexander-Webber, J. Huang, M. Saliba, I. Mora-Sero, J. Bisquert, H. J. Snaith and R. J. Nicholas, Low-temperature processed electron collection layers of graphene/TiO_2 nanocomposites in thin film perovskite solar cells, Nano Lett. 14 (2014) 724- 730 & N. G. Sahoo, Y. Pan, L. Li, S. H. Chan, Graphene-Based Materials for Energy Conversion, Adv. Mater. 24 (2012) 4203-4210.

[13] A. Subramanian, Z. Pan, G. Rong, H. Li, L. Zhou, W. Li, Y. Qiu, Y. Xu, Y. Hou, Z. Zheng, Y. Zhang, Graphene quantum dot antennas for high efficiency Förster resonance energy transfer based dye-sensitized solar cells, J. of power sources 343 (2017) 39-46.

[14] K. Habiba, V. I. Makarov, J. A., M. J. F. Guinel, B. R. Weiner, G. Morell, Luminescent graphene quantum dots fabricated by pulsed laser synthesis, Carbon 64 (2013) 341- 350.

[15] L. Kou, F. Li, W. Chen and T. Guo, Synthesis of blue light-emitting graphene quantum dots and their application in flexible nonvolatile memory, Org. Elect. 14 (2013) 1447-1451.

[16] Y. Li, Y. Hu, Y. Zhao, G. Shi, L. Deng, Y. Hou, and L. Qu, An Electrochemical Avenue to Green-Luminescent Graphene Quantum Dots as Potential Electron-Acceptors for Photovoltaics, Adv. Mater. 23 (2011) 776-780.

[17] Y. Dong, J. Shao, C. Chen, H. Li, R. Wang, Y. Chi, X. Lin and G. Chen, Blue luminescent graphene quantum dots and graphene oxide prepared by tuning the carbonization degree of citric acid. Carbon, 50 (2012) 4738- 4743.

[18] X. Yan, X. Cui, and L.-S. Li, Synthesis of Large, Stable Colloidal Graphene Quantum Dots with Tunable Size, J. Am. Chem. Soc. 132 (2010) 5944-5945.

[19] S. Zhu, J. Zhang, C. Qiao, S. Tang, Y. Li, W. Yuan, B. Li, L. Tian, F. Liu, R. Hu, H. Gao, H. Wei, H. Zhang, H. Sun and B. Yang, Strongly green-photoluminescent graphene quantum dots for bioimaging applications, Chem. Commun. 2011, 47, 6858-6860.

[20] J. Shen, Y. Zhu, X. Yang, J. Zong, J. Zhang and C. Li, One-pot hydrothermal synthesis of graphene quantum dots surface-passivated by polyethylene glycol and their photoelectric conversion under near-infrared light, New J. Chem. 36 (2012) 97-101 & D. Pan, J. Zhang, Z. Li, and M. Wu, Hydrothermal route for cutting graphene sheets into blue-luminescent graphene quantum dots, Adv. Mater. 22 (2010) 734-738.

[21] L. Tang, R. Ji, X. Cao, J. Lin, H. Jiang, X. Li, K. S. Teng, C. M. Luk, S. Zeng, J. Hao, and S. P. Lau, Deep Ultraviolet Photoluminescence of Water-Soluble Self-Passivated Graphene Quantum Dots, ACS Nano 6 (2012) 5102-5110.

[22] S. Schnez, F. Molitor, C. Stampfer, J. Güttinger, I. Shorubalko, T. Ihn, and K. Ensslin, Observation of excited states in a graphene quantum dot, Appl. Phys. Lett. 94 (2009) 012107 (3pp).

[23] L. A. Ponomarenko, F. Schedin, M. I. Katsnelson, R. Yang, E. W. Hill, K. S. Novoselov, A. K. Geim, Chaotic Dirac Billiard in Graphene Quantum Dots, Science 320 (2008) 356-358.

[24] W. S. Hummers Jr., R. E. Offeman, Preparation of Graphitic Oxide, J. Am. Chem. Soc, 80 (1958) 1339-1339.

[25] K. K. Devarepally, M-H. Hsu, A. Ivaturi, B. Chen, N. Bennett, H. M. Upadhyaya, Optimizing the room temperature binder free TiO2 paste for high efficiency flexible polymer dye sensitized solar cells, Flexible and Printed Electronics, (2019) DOI: 10.1088/2058-8585/ab02c4

[26] C. Tyagi, G. B. V. S. Lakshmi, S. Kumar, A. Tripathi, D. K. Avasthi, Structural changes in graphene oxide thin film by electron-beam irradiation. Nuclear Instruments and Methods in Physics Research B 379 (2016) 171–175.

[27] G. I. Titelman, V. Gelman, S. Bron, R. L. Khalfin, Y. Cohen, H. Bianco-Peled, Characteristics and microstructure of aqueous colloidal dispersions of graphite oxide, Carbon 43 (2005) 641-649.

[28] A. C. Ferrari, Raman spectroscopy of graphene and graphite: Disorder, electron–phonon coupling, doping and nonadiabatic effects, Solid State Commun. 143 (2007) 47–57.

[29] J. Barrera, D. Ibañez, A. Heras, V. Ruiz, A. Colina, In-situ Evidence of the Redox-State Dependence of Photoluminescence in Graphene Quantum Dots, J. Phys. Chem. Lett. 8 (2017) 531- 537.

[30] C. N. R. Rao, K. Biswas, K. S. Subrahmanyam, A. Govindaraj, Graphene, the new nanocarbon, J. Mater. Chem. 19 (2009) 2457-2469.

[31] D. Li, M. B. Müller, S. Gilje, R. B. Kaner, G. G. Wallace, Processable aqueous dispersions of graphene nanosheets, Nat. Nanotech. 3 (2008) 101-105.

[32] V. Gupta, B. K. Gupta, R.K. Kotnala, T.N. Narayanan, V. Grover, J. Shah, V. Agrawal, S. Chand, V. Shanker, Defect induced photoluminescence and ferromagnetic properties of bio-compatible SWCNT/Ni hybrid bundles, J. Colloid & Inter. Sci. 362 (2011) 311-316.

[33] M. McDowell, A. Metzger, C. Wang, J. Bao, J. M. Tour, A. A. Martí, Singular wavelength dependence on the sensitization of lanthanides by graphene quantum dots, Chem. Commun. 54 (2018) 4325-4328.

[34] S. Kim, D. H. Shin, C. O. Kim, S. S. Kang, J. M. Kim, S-H. Choi, L-H. Jin, Y.-H. Cho, S. W. Hwang and C. Sone, Size-dependent radiative decay processes in graphene quantum dots, Appl. Phys. Lett. 101 (2012) 163103.

[35] W. Wang, Z. Gu, W. Lei, W. Wang, X. Xia, Q. Hao, Graphene quantum dots as a fluorescent sensing platform for highly efficient detection of copper(II) ions, Sens. Act. Chem. B 190 (2014) 516–522.

[36] L. Kou, F. Li, W. Chen, T. Guo, Synthesis of blue light-emitting graphene quantum dots and their application in flexible nonvolatile memory, Org. Elect.14 (2013) 1447–1451.

[37] J. Barrera, D. Ibañez, A. Heras, V. Ruiz, and A. Colina, In-situ Evidence of the Redox-State Dependence of Photoluminescence in Graphene Quantum Dots, J. Phys. Chem. Lett. 8 (2017) 531- 537.

[38] D. Pan, L. Guo, J. Zhang, C. Xi, Q. Xue, H. Huang, J. Li, Z. Zhang, W. Yu, Z. Chen, Z. Li and M. Wu, Cutting sp2clusters in graphene sheets into colloidal graphene quantum dots with strong green fluorescence, J. Mater. Chem. 22 (2012) 3314- 3318.

[39] E. Lee, J. Ryu, J. Jang, Fabrication of graphene quantum dots via size-selective precipitation and their application in upconversion-based DSSCs, Chem. Commun. 49 (2013) 9995-9997.

[40] X. Fang, M. Li, K. Guo, J. Li, M. Pan, L. Bai, M. Luoshan, X. Zhao, Graphene quantum dots optimization of dye-sensitized solar cells, Electrochimi. Acta 137 (2014) 634–638.

[41] G. Zamiri, S. Bagheri, Fabrication of green dye-sensitized solar cell based on ZnO nanoparticles as a photoanode and graphene quantum dots as a photo-sensitizer, J. Colloid & Interface Sci. 511 (2018) 318–324.

[42] I. Mihalache, A. Radoi, M. Mihaila, C. Munteanu, A. Marin, M. Danila, M. Kusko, C. Kusko, Charge and energy transfer interplay in hybrid sensitized solar cells mediated by graphene quantum dots, Electrochimi. Acta 153 (2015) 306–315.

[43] Z. Salam, E. Vijayakumar, A. Subramania, N. Sivasankar, S. Mallick, Graphene quantum dots decorated electrospun TiO_2 nanofibers as an effective photoanode for dye sensitized solar cells, Solar Energy Materials & Solar Cells 143 (2015) 250–259.

[44] A. Subramanian, Z. Pan, G. Rong, H. Li, L. Zhou, W. Li, Y. Qiu, Y. Xu, Y. Hou, Z. Zheng, Y. Zhang, Graphene quantum dot antennas for high efficiency Förster resonance energy transfer based dye-sensitized solar cells, J. Power Sources, 343 (2017) 39-46.

[45] S. Kundu, P. Sarojinijeeva, R. Karthick, G. Anantharaj, G. Saritha, R. Bera, S. Anandand, A. Patra, P. Ragupathy, M. Selvaraj, D. Jeyakumar, K. V. Pillai, Enhancing the Efficiency of DSSCs by the Modification of TiO_2 photoanodes using N, F and S, co-doped graphene quantum dots, Electrochimi. Acta 242 (2017) 337–343.

[46] A. Maity, A. Kuila, S. Das, D. Mandal, A. Shit, A. K. Nandi, Optoelectronic and photovoltaic properties of graphene quantum dot–polyaniline nanostructures, J. Mater. Chem. A 3 (2015) 20736-20748.

[47] P. Routh, S. Das, A. Shit, P. Bairi, P. Das, A. K. Nandi, Graphene Quantum Dots from a Facile Sono-Fenton Reaction and Its Hybrid with a Polythiophene Graft Copolymer toward Photovoltaic Application, ACS Appl. Mater. Interfaces 5 (2013) 12672−12680.

[48] Q. Wang, J. E. Moser and M. Gratzel, Electrochemical impedance spectroscopic analysis of dye-sensitized solar cells, J. Phys. Chem. B 109 (2005) 14945- 14953.

[49] S. P. Singh, K. S. V. Gupta, G. D. Sharma, A. Islam, L. Han, Efficient thiocyanate-free sensitizer: a viable alternative to N719 dye for dye-sensitized solar cells. Dalton Trans. 41 (2012) 7604-7608.

[50] A. Mathew, G. M. Rao, N. Munichandraiah, Effect of TiO_2 electrode thickness on photovoltaic properties of dye sensitized solar cell based on randomly oriented Titania nanotubes, Mater. Chem. Phys. 127 (2011) 95-101.

[51] A. C. Fisher, L. M. Peter, E. A. Ponomarev, A. B. Walker and K. G. U. Wijayantha, Intensity dependence of the back reaction and transport of electrons in dye-sensitized nanocrystalline TiO_2 solar Cells, J. Phys. Chem. B 104 (2000) 949-958.

List of Figures

Fig. 1: X-ray diffraction (XRD) pattern of GO [$2\theta = 9.48°$ corresponds to the (001) planes], rGO [$2\theta = 26.3°$ corresponds to the (002) planes] and GQDs ($2\theta = 26.11°$ corresponds to the (002) planes].

Fig. 2: Raman spectrum of GO and rGO represents D band at 1351 cm^{-1} and G band at 1592 cm^{-1}.

Fig. 3: UV-Vis absorption spectrum of GQDs exhibiting characteristic hump at 270nm.

Fig. 4: Photoluminescence spectra of GQDs in water excited at wavelengths from 300 nm to 372 nm with intervals of 8 nm.

Fig. 5: Life time decay studies of GQDs in DI water.

Fig. 6: SEM micrographs of rGO a) lower magnification b) higher magnification images, ripples on the surface of rGO indicate the presence of surface defects due to oxygen vacancies.

Fig. 7: HRTEM micrographs of GQDs and inset indicate the dots of size 2-3 nm.

Fig. 8: J-V characteristics of flexible solar cell made with binder free GQD-TiO_2 paste (red curve in presence of light and black in dark condition) and TiO_2 paste (dark cyan curve in presence of light and blue in the dark) recorded under simulated AM1.5G.

Fig. 9: Nyquist plots of GQDs-TiO_2 (red colour) and TiO_2 (black colour) cells measured at -0.7 V in dark condition.

Fig. 10: Bode-modulus phase plots of GQDs-TiO_2 and TiO_2 cells recorded at -0.7V under dark conditions.

List of tables

Table.1: Photovoltaic performances of DSSCs devices fabricated with GQDs as photoelectrode.